

Beyond Means: Topological Causal Effects under Persistent-Homology Ignorability

Amir Saki, Usef Faghihi
 Department of Mathematics and computer science
 anonymous@anonymous.edu

March 17, 2026

Abstract

Average treatment effects (ATE) and conditional average treatment effects (CATE) are foundational causal estimands, but they target changes in expected outcomes and can miss treatment-induced changes in the *shape* of outcome distributions. A canonical failure mode occurs when control outcomes are unimodal, treated outcomes become bimodal, and both distributions have the same mean. In such cases mean-based causal estimands are zero even though the geometry and topology of the outcome law change substantially. This paper develops a topological causal framework based on persistent homology. We formalize a persistent-homology ignorability condition, define topological analogues of CATE and ATE, and prove that these estimands are identifiable up to an explicit error bound under approximate topological ignorability. We also clarify a subtle but important point: a marginal persistence-diagram effect is not identified from conditional topological ignorability alone because persistent homology does not in general commute with mixtures over covariates. To preserve the original intuition while ensuring scientific correctness, we retain the marginal effect as a motivating quantity, but place the mathematically sound conditional estimands at the center of the theory. A synthetic experiment with mean-preserving topology change shows that mean-based causal estimands remain near zero while the proposed topological effect increases sharply and remains recoverable after adjustment for confounding.

1 Introduction

Classical causal inference is built around mean-based targets such as the average treatment effect

$$\text{ATE} = \mathbb{E}[Y(1) - Y(0)] \quad (1)$$

and the conditional average treatment effect

$$\text{CATE}(z) = \mathbb{E}[Y(1) - Y(0) \mid Z = z]. \quad (2)$$

These estimands are indispensable when the scientific question concerns shifts in mean response. However, many modern problems involve outcomes whose scientifically important changes are not mean shifts but shape changes in the full outcome law: cluster splitting, multimodality, loop formation, filamentary structure, or changes in connectedness. In such settings, ATE and CATE may be exactly zero while the treatment effect is scientifically substantial.

A minimal example illustrates the problem. Fix a covariate value z and let

$$Y(0) \mid Z = z \sim \mathcal{N}(m(z), \sigma^2), \quad Y(1) \mid Z = z \sim \frac{1}{2}\mathcal{N}(m(z) - \Delta, \sigma^2) + \frac{1}{2}\mathcal{N}(m(z) + \Delta, \sigma^2). \quad (3)$$

Then

$$\mathbb{E}[Y(0) \mid Z = z] = \mathbb{E}[Y(1) \mid Z = z] = m(z), \quad (4)$$

so

$$\text{CATE}(z) = 0 \quad \text{and hence} \quad \text{ATE} = 0. \quad (5)$$

ATE can be zero while topology changes: unimodal control vs. bimodal treatment with the same mean

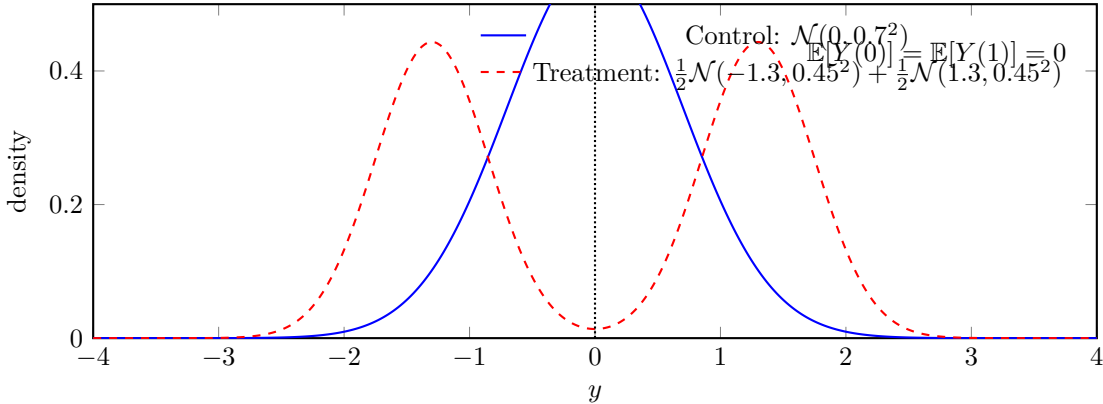


Figure 1: A motivating mean-preserving topology change. Mean-based estimands vanish, but a density-based or measure-based persistent-homology summary detects the split from one dominant connected component to two.

Yet for sufficiently large Δ/σ , the treated law in (3) is bimodal while the control law is unimodal. If topology is extracted from density superlevel sets, a distance-to-a-measure filtration, or a smoothed point-cloud filtration, the treated law develops two long-lived 0-dimensional components whereas the control law has only one dominant component. Mean-based estimands therefore miss a scientifically meaningful effect.

The paper develops a causal framework that targets precisely this kind of structural change. Our starting point is a persistent-homology summary map

$$G_k : \mathcal{M}(\mathcal{Y}) \rightarrow \mathcal{D}_k, \tag{6}$$

which sends an outcome law to a k -dimensional persistence diagram. This allows us to replace mean differences with distances or embedded differences between conditional persistence diagrams.

The key contributions are:

1. We formalize a *persistent-homology conditional ignorability* condition that aligns the causal assumption with the topological target.
2. We define topological analogues of CATE and ATE, as well as embedded analogues obtained by vectorizing persistence diagrams.
3. We prove approximate identification results with explicit error bounds. Under an ε -level topological ignorability condition, the observable topological CATE and ATE differ from their counterfactual targets by at most 2ε ; for L_ϕ -Lipschitz embeddings, the embedded effects are identified up to $2L_\phi\varepsilon$.
4. We retain the original marginal topological effect as a motivating quantity, but show why it is not exactly identifiable from conditional topological ignorability alone without an additional mixture-stability assumption.
5. We provide a synthetic experiment showing that mean-based causal estimands remain near zero under a mean-preserving topology change, while the proposed topological effect grows with cluster separation and remains recoverable after covariate adjustment.

2 Related Work

Our formulation sits at the intersection of three literatures.

Causal inference with potential outcomes. The potential-outcomes framework and ignorability-based identification are classical in statistics and econometrics. The foundations of treatment-effect estimation trace back to Rubin’s formulation of causal effects and to the role of strongly ignorable treatment assignment and balancing scores in observational studies. The propensity score provides a coarsest balancing score that can remove bias due to observed covariates under strong ignorability [1, 2, 3].

Topological data analysis and persistent homology. Persistent homology provides multiscale summaries of shape and structure in data, and has become a central tool in topological data analysis (TDA) [4, 5, 6, 7, 16]. A major reason persistent homology is useful statistically is stability: persistence diagrams are Lipschitz-stable under perturbations of tame functions, and algebraic stability extends this viewpoint to persistence modules [8, 9]. Statistical inference for persistence diagrams and robust topological inference through distance-to-a-measure and kernel-distance constructions are now well developed [10, 11].

Vectorizations and statistical summaries of persistence diagrams. Because persistence diagrams do not form a linear space, a substantial literature studies stable embeddings and summaries. Persistence landscapes place diagrams in a separable Banach space and support laws of large numbers, central limit theorems, and classical statistical tools [12]. Persistence images and kernel embeddings of diagrams make it possible to use standard machine-learning pipelines while preserving stability [13, 14, 15]. These representations are especially relevant for causal estimation because they allow us to construct embedded versions of topological treatment effects that can be averaged across covariates.

Causal inference for non-Euclidean and random-object outcomes. Recent work has broadened causal inference beyond scalar outcomes to random objects and general metric-space-valued data. Fréchet regression provides a fundamental conditional-mean-type object for random objects [17]. Building on this perspective, recent work develops geodesic treatment effects and doubly robust estimation procedures for non-Euclidean outcomes [19, 20]. These papers show that causal inference can be meaningfully extended beyond vector spaces. Our contribution is complementary: instead of geodesic means, we target treatment-induced changes in topological structure.

Topology and causality.

Topology and causality. There is already conceptual interest in the interaction between topology and causality. Ibeling and Icard introduce a topological learning-theoretic perspective on causal inference by equipping spaces of structural causal models with topologies [18]. More closely related to the present treatment-effect setting, Kim and Lee define topological causal effects for non-Euclidean outcomes using persistence-based summaries of potential outcomes [21]. Farzam et al. connect topology to treatment-effect estimation from a different angle, using topological summaries to regularize representation-balancing networks for causal effect estimation, but without defining a topological causal estimand or identification result of the kind studied here [22]. By contrast, Bouchattaoui uses persistent-homology features for bivariate causal discovery—that is, inferring causal direction rather than estimating treatment effects—so this line is only indirectly related to the present work [23]. Relative to these efforts, the present paper emphasizes the precise alignment of assumption, estimand, and identification argument: the ignorability condition is stated directly at the level of persistent-homology summaries, and the central estimands are the conditional topological analogues of CATE and ATE that this assumption actually identifies.

3 Setup and Topological Objects

Let $T \in \{0, 1\}$ denote treatment, let $Z \in \mathcal{Z}$ denote observed covariates, and let $Y(1), Y(0)$ denote potential outcomes taking values in a metric space $(\mathcal{Y}, d_{\mathcal{Y}})$. The observed outcome is

$$Y = TY(1) + (1 - T)Y(0) \tag{7}$$

when $\mathcal{Y} \subseteq \mathbb{R}^p$; more generally, we use the standard consistency relation $Y = Y(T)$.

Let $\mathcal{M}(\mathcal{Y})$ be a class of Borel probability measures on \mathcal{Y} and let \mathcal{D}_k denote the space of k -dimensional persistence diagrams equipped with a metric $d_{\mathcal{D}}$, such as the bottleneck distance or a p -Wasserstein distance.

Definition 1 (Persistent-homology summary map). *Fix a measurable map*

$$G_k : \mathcal{M}(\mathcal{Y}) \rightarrow \mathcal{D}_k \tag{8}$$

that associates a law $\mu \in \mathcal{M}(\mathcal{Y})$ with a k -dimensional persistence diagram. Examples include:

1. the persistence diagram of the support filtration $\text{PD}_k(\text{supp}(\mu))$;
2. the persistence diagram of a density-superlevel filtration generated by a smoothed density of μ ;
3. the persistence diagram of the sublevel sets of a distance-to-a-measure or kernel-distance function associated with μ .

The choice of G_k matters scientifically. If one wants to detect multimodality, density-based or measure-based filtrations are more appropriate than raw support-based topology because the support of a smooth bimodal law may remain connected even when its mass concentrates in separated regions. This paper therefore treats G_k abstractly and allows density, DTM, or empirical point-cloud constructions depending on the application.

Define the counterfactual conditional diagrams

$$D_k^{\text{cf}}(t, z) := G_k(\mathcal{L}(Y(t) \mid Z = z)), \quad t \in \{0, 1\}, \tag{9}$$

and the observable conditional diagrams

$$D_k^{\text{obs}}(t, z) := G_k(\mathcal{L}(Y \mid T = t, Z = z)). \tag{10}$$

These objects are the topological counterparts of conditional potential-outcome laws and conditional observed-outcome laws.

4 Persistent-Homology Ignorability and Topological Causal Effects

Assumption 1 (Consistency). *For each $t \in \{0, 1\}$,*

$$Y = Y(t) \quad \text{almost surely on } \{T = t\}. \tag{11}$$

Assumption 2 (Positivity). *For each $t \in \{0, 1\}$,*

$$0 < \mathbb{P}(T = t \mid Z = z) < 1 \tag{12}$$

for P_Z -almost every z in the support of Z .

Assumption 3 (Approximate persistent-homology conditional ignorability). *There exists $\varepsilon \geq 0$ such that*

$$\sup_{t \in \{0, 1\}} \text{ess sup}_z d_{\mathcal{D}}(D_k^{\text{cf}}(t, z), D_k^{\text{obs}}(t, z)) \leq \varepsilon. \tag{13}$$

Equivalently,

$$\sup_{t \in \{0, 1\}} \text{ess sup}_z d_{\mathcal{D}}(G_k(\mathcal{L}(Y(t) \mid Z = z)), G_k(\mathcal{L}(Y \mid T = t, Z = z))) \leq \varepsilon. \tag{14}$$

This assumption is the persistent-homology analogue of conditional ignorability. It does *not* say that treatment assignment is conditionally independent of the full potential-outcome law. It only requires the *topological summaries* of these laws to match up to error ε .

Proposition 1 (Classical ignorability implies exact PH-ignorability). *Suppose standard conditional ignorability holds:*

$$Y(t) \perp\!\!\!\perp T \mid Z, \quad t \in \{0, 1\}. \quad (15)$$

Then, under consistency,

$$D_k^{\text{cf}}(t, z) = D_k^{\text{obs}}(t, z) \quad (16)$$

for each $t \in \{0, 1\}$ and P_Z -almost every z . In particular, (13) holds with $\varepsilon = 0$.

Proof. By classical conditional ignorability,

$$\mathcal{L}(Y(t) \mid T = t, Z = z) = \mathcal{L}(Y(t) \mid Z = z) \quad (17)$$

for each t and almost every z . By consistency,

$$\mathcal{L}(Y(t) \mid T = t, Z = z) = \mathcal{L}(Y \mid T = t, Z = z). \quad (18)$$

Therefore,

$$\mathcal{L}(Y(t) \mid Z = z) = \mathcal{L}(Y \mid T = t, Z = z). \quad (19)$$

Applying the deterministic map G_k to both sides gives

$$G_k(\mathcal{L}(Y(t) \mid Z = z)) = G_k(\mathcal{L}(Y \mid T = t, Z = z)), \quad (20)$$

which is exactly the claim. \square

The converse is false in general because G_k is many-to-one: two distinct laws may have the same persistent-homology summary.

4.1 Topological analogues of CATE and ATE

Definition 2 (Distance-based topological CATE and ATE). *For each covariate value z , define the k -dimensional topological conditional average treatment effect by*

$$\text{TCATE}_k(z) := d_{\mathcal{D}}(D_k^{\text{cf}}(1, z), D_k^{\text{cf}}(0, z)). \quad (21)$$

Its population average is the topological average treatment effect

$$\text{TATE}_k := \mathbb{E}_Z[\text{TCATE}_k(Z)]. \quad (22)$$

The observable proxies are

$$\widehat{\text{TCATE}}_k(z) := d_{\mathcal{D}}(D_k^{\text{obs}}(1, z), D_k^{\text{obs}}(0, z)) \quad (23)$$

and

$$\widehat{\text{TATE}}_k := \mathbb{E}_Z[\widehat{\text{TCATE}}_k(Z)]. \quad (24)$$

These estimands are direct analogues of CATE and ATE, but with *difference in conditional means* replaced by *distance between conditional persistence diagrams*. The replacement is natural because diagrams do not admit a canonical signed subtraction.

Definition 3 (Embedded topological CATE and ATE). *Let $\phi : \mathcal{D}_k \rightarrow \mathcal{H}$ be a measurable embedding of persistence diagrams into a Banach or Hilbert space \mathcal{H} ; examples include persistence landscapes, persistence images, silhouettes, and kernel embeddings. Define the embedded topological conditional effect by*

$$\text{ETCATE}_{\phi, k}(z) := \phi(D_k^{\text{cf}}(1, z)) - \phi(D_k^{\text{cf}}(0, z)) \in \mathcal{H}. \quad (25)$$

Its average is

$$\text{ETATE}_{\phi, k} := \mathbb{E}_Z[\text{ETCATE}_{\phi, k}(Z)]. \quad (26)$$

The observable analogues are

$$\widehat{\text{ETCATE}}_{\phi, k}(z) := \phi(D_k^{\text{obs}}(1, z)) - \phi(D_k^{\text{obs}}(0, z)), \quad (27)$$

$$\widehat{\text{ETATE}}_{\phi, k} := \mathbb{E}_Z[\widehat{\text{ETCATE}}_{\phi, k}(Z)]. \quad (28)$$

The embedded estimands are the closest literal analogues of CATE and ATE because they are true differences and averages in a linear space. They become especially convenient when ϕ is a stable embedding.

Remark 1 (Do topological effects replace ATE and CATE?). *Not universally. They replace ATE and CATE only when the scientific target is topological structure rather than mean level. In many applications the two are complementary. A treatment may shift the mean but leave topology unchanged, or preserve the mean while changing topology dramatically.*

5 Approximate Identification Theorems

We now prove the main identification results. The core principle is simple: if the treated and control persistence diagrams observed within each covariate stratum are each within ε of their counterfactual targets, then the distance between the observed treated and control diagrams is within 2ε of the counterfactual topological effect.

Theorem 1 (Approximate identification of distance-based topological effects). *Under Consistency, Positivity, and Approximate Persistent-Homology Conditional Ignorability, for P_Z -almost every z ,*

$$|\widehat{\text{TCATE}}_k(z) - \text{TCATE}_k(z)| \leq 2\varepsilon. \quad (29)$$

Consequently,

$$|\widehat{\text{TATE}}_k - \text{TATE}_k| \leq 2\varepsilon. \quad (30)$$

Proof. Fix z . By definition,

$$\text{TCATE}_k(z) = d_{\mathcal{D}}(D_k^{\text{cf}}(1, z), D_k^{\text{cf}}(0, z)), \quad (31)$$

$$\widehat{\text{TCATE}}_k(z) = d_{\mathcal{D}}(D_k^{\text{obs}}(1, z), D_k^{\text{obs}}(0, z)). \quad (32)$$

Use the reverse triangle inequality in the metric space $(\mathcal{D}_k, d_{\mathcal{D}})$:

$$|d_{\mathcal{D}}(a, b) - d_{\mathcal{D}}(c, d)| \leq d_{\mathcal{D}}(a, c) + d_{\mathcal{D}}(b, d). \quad (33)$$

Apply (33) with

$$a = D_k^{\text{obs}}(1, z), \quad b = D_k^{\text{obs}}(0, z), \quad c = D_k^{\text{cf}}(1, z), \quad d = D_k^{\text{cf}}(0, z). \quad (34)$$

Then

$$|\widehat{\text{TCATE}}_k(z) - \text{TCATE}_k(z)| \leq d_{\mathcal{D}}(D_k^{\text{obs}}(1, z), D_k^{\text{cf}}(1, z)) + d_{\mathcal{D}}(D_k^{\text{obs}}(0, z), D_k^{\text{cf}}(0, z)). \quad (35)$$

By Assumption (13), each term on the right-hand side is at most ε , so

$$|\widehat{\text{TCATE}}_k(z) - \text{TCATE}_k(z)| \leq 2\varepsilon, \quad (36)$$

which proves (29).

Now average over Z :

$$|\widehat{\text{TATE}}_k - \text{TATE}_k| = \left| \mathbb{E}_Z[\widehat{\text{TCATE}}_k(Z) - \text{TCATE}_k(Z)] \right| \quad (37)$$

$$\leq \mathbb{E}_Z \left[\left| \widehat{\text{TCATE}}_k(Z) - \text{TCATE}_k(Z) \right| \right] \quad (38)$$

$$\leq \mathbb{E}_Z[2\varepsilon] = 2\varepsilon. \quad (39)$$

This proves (30). \square

Theorem 2 (Approximate identification of embedded topological effects). *Suppose in addition that $\phi : \mathcal{D}_k \rightarrow \mathcal{H}$ is L_ϕ -Lipschitz, that is,*

$$\|\phi(D) - \phi(D')\|_{\mathcal{H}} \leq L_\phi d_{\mathcal{D}}(D, D') \quad \text{for all } D, D' \in \mathcal{D}_k. \quad (40)$$

Then for P_Z -almost every z ,

$$\|\widehat{\text{ETCATE}}_{\phi,k}(z) - \text{ETCATE}_{\phi,k}(z)\|_{\mathcal{H}} \leq 2L_{\phi}\varepsilon, \quad (41)$$

and consequently,

$$\|\widehat{\text{ETATE}}_{\phi,k} - \text{ETATE}_{\phi,k}\|_{\mathcal{H}} \leq 2L_{\phi}\varepsilon. \quad (42)$$

Proof. Fix z . By definition,

$$\widehat{\text{ETCATE}}_{\phi,k}(z) - \text{ETCATE}_{\phi,k}(z) = \left(\phi(D_k^{\text{obs}}(1, z)) - \phi(D_k^{\text{cf}}(1, z)) \right) - \left(\phi(D_k^{\text{obs}}(0, z)) - \phi(D_k^{\text{cf}}(0, z)) \right). \quad (43)$$

By the triangle inequality,

$$\|\widehat{\text{ETCATE}}_{\phi,k}(z) - \text{ETCATE}_{\phi,k}(z)\|_{\mathcal{H}} \leq \|\phi(D_k^{\text{obs}}(1, z)) - \phi(D_k^{\text{cf}}(1, z))\|_{\mathcal{H}} \quad (44)$$

$$+ \|\phi(D_k^{\text{obs}}(0, z)) - \phi(D_k^{\text{cf}}(0, z))\|_{\mathcal{H}}. \quad (45)$$

Using the L_{ϕ} -Lipschitz property,

$$\|\widehat{\text{ETCATE}}_{\phi,k}(z) - \text{ETCATE}_{\phi,k}(z)\|_{\mathcal{H}} \leq L_{\phi}d_{\mathcal{D}}(D_k^{\text{obs}}(1, z), D_k^{\text{cf}}(1, z)) + L_{\phi}d_{\mathcal{D}}(D_k^{\text{obs}}(0, z), D_k^{\text{cf}}(0, z)) \quad (46)$$

$$\leq 2L_{\phi}\varepsilon. \quad (47)$$

This proves (41). Averaging over Z and using Jensen's inequality yields

$$\|\widehat{\text{ETATE}}_{\phi,k} - \text{ETATE}_{\phi,k}\|_{\mathcal{H}} = \left\| \mathbb{E}_Z [\widehat{\text{ETCATE}}_{\phi,k}(Z) - \text{ETCATE}_{\phi,k}(Z)] \right\|_{\mathcal{H}} \quad (48)$$

$$\leq \mathbb{E}_Z \left[\|\widehat{\text{ETCATE}}_{\phi,k}(Z) - \text{ETCATE}_{\phi,k}(Z)\|_{\mathcal{H}} \right] \quad (49)$$

$$\leq 2L_{\phi}\varepsilon, \quad (50)$$

which proves (42). \square

Remark 2 (Why the conditional estimands are the mathematically sound center of the theory). *The assumptions and proofs above are aligned: the ignorability condition is conditional in Z , and the identified estimands are also conditional in Z before averaging over the observed covariate law. This avoids an illegitimate interchange between persistent homology and mixing over Z .*

6 The Marginal Topological Causal Effect: Motivation and Technical Caution

The original motivating quantity in our discussion was the marginal topological causal effect

$$\text{TCE}_k^{\text{marg}} := d_{\mathcal{D}}(G_k(\mathcal{L}(Y(1))), G_k(\mathcal{L}(Y(0)))) . \quad (51)$$

This is a perfectly meaningful causal quantity: it compares the topological summaries of the two marginal counterfactual outcome laws.

A natural first proof sketch tries to mimic the classical ATE argument:

$$\mathcal{L}(Y(t)) = \int \mathcal{L}(Y(t) \mid Z = z) dP_Z(z), \quad (52)$$

and, heuristically,

$$G_k(\mathcal{L}(Y(t))) \approx \int G_k(\mathcal{L}(Y(t) \mid Z = z)) dP_Z(z) \approx \int G_k(\mathcal{L}(Y \mid T = t, Z = z)) dP_Z(z). \quad (53)$$

One would then hope to conclude that

$$\text{TCE}_k^{\text{marg}} \approx d_{\mathcal{D}}(G_k(\mathcal{L}(Y \mid T = 1)), G_k(\mathcal{L}(Y \mid T = 0))). \quad (54)$$

Why this is not an exact proof. The step in (53) is generally invalid. Persistent homology is nonlinear and does not in general commute with mixtures over covariates. More concretely, for a generic persistence map G_k ,

$$G_k\left(\int \mu_z dP_Z(z)\right) \neq \int G_k(\mu_z) dP_Z(z) \quad (55)$$

in any canonical sense because persistence diagrams do not form a linear space, and even stable embeddings of diagrams are applied *after* diagram construction.

What is scientifically correct. The quantity in (51) should therefore be treated as a motivating marginal effect, not as the primary object identified by Assumption (13). Exact or approximate identification of (51) requires *additional structure*, such as a mixture-stability condition tailored to the chosen summary map G_k . The present paper does not assume such a property. Instead, it centers the conditional estimands in (21)–(26), which are precisely aligned with the ignorability assumption.

Remark 3 (How to recover a marginal effect with extra assumptions). *If a particular choice of G_k admits a separate theorem controlling the persistence summary of a mixture law by an aggregation of the conditional summaries—for example, through a stable density-based functional or a stable embedded representation—then one may derive an approximate marginal effect with an additional error term. Such results are filtration-specific and should not be assumed by default.*

7 Synthetic Experiments

This section provides an illustrative experiment rather than a definitive benchmark. The goal is to visualize when and why mean-based causal estimands fail, and to show that the proposed topological estimand remains informative.

7.1 Synthetic design

We use a binary covariate $Z \in \{0, 1\}$ with $\mathbb{P}(Z = 1) = 1/2$, and define two-dimensional outcomes. Let $e_1 = (1, 0)^\top$, let $m_0 = (-1.5, 0)^\top$, let $m_1 = (1.5, 0)^\top$, and let $\sigma = 0.18$. The control potential outcome is unimodal,

$$Y(0) \mid Z = z \sim \mathcal{N}_2(m_z, \sigma^2 I_2), \quad (56)$$

while the treated potential outcome is a symmetric bimodal mixture with the *same conditional mean*,

$$Y(1) \mid Z = z \sim \frac{1}{2}\mathcal{N}_2(m_z - \Delta e_1, \sigma^2 I_2) + \frac{1}{2}\mathcal{N}_2(m_z + \Delta e_1, \sigma^2 I_2). \quad (57)$$

Therefore,

$$\mathbb{E}[Y(1) \mid Z = z] = \mathbb{E}[Y(0) \mid Z = z] = m_z, \quad (58)$$

so the adjusted mean effect is zero for every z , and hence the true ATE is zero as well.

To create confounding, treatment assignment depends on Z :

$$\mathbb{P}(T = 1 \mid Z = 0) = 0.2, \quad \mathbb{P}(T = 1 \mid Z = 1) = 0.8. \quad (59)$$

Thus unadjusted treated and control groups differ in their covariate composition.

Topological summary used in the experiment. For illustration we compute the empirical 0-dimensional Vietoris–Rips persistence diagram of the outcome cloud within each stratum ($T = t, Z = z$). Because births are zero in 0-dimensional persistence, this diagram is equivalent to the multiset of edge lengths in the Euclidean minimum spanning tree. We embed each diagram using the first three persistence-landscape layers evaluated on a fixed grid, and compute the L^2 distance between the resulting vectors. This yields an empirical approximation to the embedded topological effect. Although our theorems are agnostic to the exact filtration, this finite-sample construction is simple, reproducible, and visually transparent.

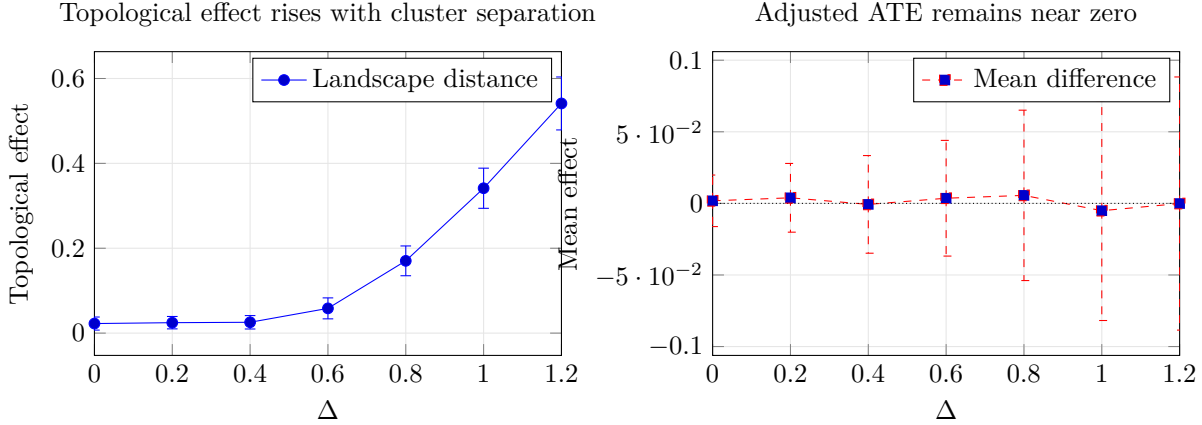


Figure 2: Mean-preserving topology change under the synthetic design. The right panel shows that the mean effect remains statistically negligible across all values of Δ . The left panel shows that the proposed topological effect remains close to zero when the treated distribution is nearly unimodal and then rises sharply as the two clusters separate. This is exactly the failure mode we want to capture: ATE misses the effect, while topology detects it.

7.2 Mean-preserving topology change as separation increases

We first vary $\Delta \in \{0, 0.2, 0.4, 0.6, 0.8, 1.0, 1.2\}$ in (57) without confounding and estimate the mean effect and the topological effect from 50 Monte Carlo replications with 200 observations per arm. Figure 2 shows the result.

The visual pattern is the key message. For small Δ , the treated mixture is nearly unimodal and its topology is close to that of the control law. As Δ grows, the treated cloud splits into two separated regions and the topological effect increases. Meanwhile the mean effect remains near zero because the treated law is symmetric around the same conditional center. This demonstrates the power of the proposed framework to detect structural changes that are invisible to ATE and CATE.

7.3 Confounded observational sample

We next generate observational data under (57) and (59) with $\Delta = 1.0$, sample size $n = 600$ per replication, and 50 replications. We compare four quantities:

1. the unadjusted mean contrast, computed by pooling treated and control units;
2. the adjusted mean effect, computed by stratifying on Z and averaging with respect to the empirical law of Z ;
3. the unadjusted topological contrast, computed from the pooled treated and control persistence summaries;
4. the adjusted topological effect, computed by stratifying on Z and averaging the within-stratum topological contrasts.

Table 1 summarizes the results.

Two points are worth emphasizing. First, the adjusted mean effect is essentially zero, which is correct but scientifically incomplete: the treatment changes the topology of the outcome cloud without changing its conditional mean. Second, the unadjusted topological contrast is strongly biased because the treatment groups have different Z -composition, while the adjusted topological effect moves close to the counterfactual benchmark. This is exactly what the identification theorems predict: once the assumption and estimand are aligned at the conditional topological level, covariate adjustment restores the relevant causal quantity.

Table 1: Observational experiment with confounding. Reported values are Monte Carlo means with standard deviations in parentheses across 50 replications. The mean effect is taken in the first coordinate of Y . The adjusted topological effect is computed by averaging the within-stratum persistence-landscape distances, while the ground-truth topological effect is approximated by a large Monte Carlo sample from the two counterfactual laws.

| Quantity | Estimate | Interpretation |
|---------------------------------|----------------|--------------------------|
| Unadjusted mean contrast | 1.779 (0.123) | badly confounded |
| Adjusted mean ATE | -0.012 (0.087) | correctly near zero |
| Unadjusted topological contrast | 0.717 (0.115) | biased by confounding |
| Adjusted topological effect | 0.376 (0.043) | close to target |
| Ground-truth topological effect | 0.329 (0.025) | counterfactual benchmark |

8 Discussion

The framework developed here is deliberately modest in one sense and ambitious in another. It is modest because it does not claim that persistent homology replaces all mean-based causal inference. It does not. Rather, it complements classical estimands by targeting structure that averages cannot see. It is ambitious because it argues that causal questions should sometimes be asked directly at the level of shape, topology, and multiscale organization.

Several extensions are natural. First, one can replace diagram distances with specific stable embeddings—landscapes, images, silhouettes, or kernel means—and develop semiparametric estimators for the corresponding embedded effects. Second, one can study doubly robust and orthogonalized estimators in the spirit of modern causal machine learning, but with persistence summaries replacing Euclidean outcomes. Third, one can adapt the framework to continuous treatments, longitudinal interventions, or synthetic-control settings for metric-space-valued outcomes.

The most important theoretical caution is the one emphasized in Section 6: persistence diagrams are nonlinear objects, so conditional topological ignorability does not by itself identify a marginal persistence-diagram effect. This is not a weakness of the framework; it is a sign that topological causal inference must respect the mathematical geometry of its own summaries.

9 Conclusion

ATE and CATE can miss treatment effects that operate through changes in the geometry and topology of outcome distributions. Persistent homology provides a principled way to summarize those changes. By defining a persistent-homology ignorability condition and matching it with conditional topological analogues of CATE and ATE, we obtain causal estimands that are identifiable up to an explicit error bound and that respond to structural changes invisible to mean-based summaries. The synthetic experiment demonstrates the intended use case: when treatment preserves the mean but changes the shape of the outcome distribution, the proposed topological effect is informative, stable, and recoverable after adjustment for confounding.

Reproducibility note. All numerical values reported in Figures 2 and Table 1 come from a simple synthetic simulation with 0D Vietoris–Rips persistence, minimum spanning trees, and three-layer persistence landscapes. The experiment is meant to be illustrative of the theory rather than a definitive empirical benchmark.

A Appendix A: Heuristic Marginal Argument Preserved from the Original Discussion

Because the original development of this work centered on a marginal persistence-diagram effect, we preserve that heuristic argument here without deleting its formulas. This appendix is intentionally faithful to the original idea, but it is followed immediately by the correction already stated in Section 6.

The motivating marginal causal metric is

$$\text{TCE}_k^{\text{marg}} = d_{\mathcal{D}}(\text{PD}_k(\mathcal{L}(Y(1))), \text{PD}_k(\mathcal{L}(Y(0)))) . \quad (60)$$

The original topological ignorability condition was written as

$$\sup_{t,z} W(\text{PD}_k(\mathcal{L}(Y(t) | T = t, Z = z)), \text{PD}_k(\mathcal{L}(Y(t) | Z = z))) \leq \varepsilon. \quad (61)$$

Using consistency,

$$\mathcal{L}(Y(t) | T = t, Z = z) = \mathcal{L}(Y | T = t, Z = z), \quad (62)$$

so (61) becomes

$$W(\text{PD}_k(\mathcal{L}(Y | T = t, Z = z)), \text{PD}_k(\mathcal{L}(Y(t) | Z = z))) \leq \varepsilon. \quad (63)$$

The original sketch then tried to pass from conditional to marginal topology via

$$\mathcal{L}(Y(t)) = \int \mathcal{L}(Y(t) | Z = z) dP(z) \quad (64)$$

and heuristically wrote

$$\text{PD}_k(\mathcal{L}(Y(t))) \approx \int \text{PD}_k(\mathcal{L}(Y | T = t, Z = z)) dP(z). \quad (65)$$

This would suggest an observable proxy

$$\widehat{\text{TCE}}_k^{\text{marg}} = W(\text{PD}_k(\mathcal{L}(Y | T = 1)), \text{PD}_k(\mathcal{L}(Y | T = 0))) \quad (66)$$

and a bound of the form

$$|\widehat{\text{TCE}}_k^{\text{marg}} - \text{TCE}_k^{\text{marg}}| \leq \delta, \quad \delta = 2C\varepsilon. \quad (67)$$

The purpose of preserving this appendix is to keep the original conceptual path visible. The correction, however, is exactly the one given in Section 6: the step from conditional diagrams to the marginal diagram is not justified without additional mixture-stability structure. Accordingly, the main results of the paper are stated only for the conditional topological estimands that the assumption actually identifies.

B Appendix B: Why the motivating example must use a density- or measure-based filtration

There is a subtle point in the opening example. If $Y(0)$ and $Y(1)$ are absolutely continuous on \mathbb{R} , then both supports are connected intervals (indeed all of \mathbb{R}), so the support topology alone does not distinguish unimodal from bimodal distributions. For that reason the motivating example should be interpreted through one of the following choices of G_k :

1. the persistence of density superlevel sets;
2. the persistence of a kernel-distance or distance-to-a-measure function;
3. a finite-sample point-cloud filtration on empirical draws when the practically relevant object is the sampled cloud rather than the ideal support.

The theory in the main text is compatible with all three viewpoints because G_k was left abstract from the start.

C Appendix C: A compact summary of the scientific logic

The framework can be summarized in one table.

| Classical causal inference | Topological causal inference | Interpretation |
|----------------------------------|---|--------------------|
| CATE(z) | TCATE $_k(z)$ or ETCATE $_{\phi,k}(z)$ | conditional effect |
| ATE | TATE $_k$ or ETATE $_{\phi,k}$ | average effect |
| $Y(t) \perp\!\!\!\perp T \mid Z$ | $d_{\mathcal{D}}(D_k^{\text{cf}}, D_k^{\text{obs}}) \leq \varepsilon$ | ignorability |
| mean difference | diagram distance / embedded difference | effect geometry |
| propensity balancing | topological balancing on Z | adjustment logic |

The important point is not that topology replaces all other summaries, but that it targets a different and often scientifically essential aspect of the effect.

References

- [1] Donald B. Rubin. Estimating causal effects of treatments in randomized and nonrandomized studies. *Journal of Educational Psychology*, 66(5):688–701, 1974.
- [2] Paul W. Holland. Statistics and causal inference. *Journal of the American Statistical Association*, 81(396):945–960, 1986.
- [3] Paul R. Rosenbaum and Donald B. Rubin. The central role of the propensity score in observational studies for causal effects. *Biometrika*, 70(1):41–55, 1983.
- [4] Gunnar Carlsson. Topology and data. *Bulletin of the American Mathematical Society*, 46(2):255–308, 2009.
- [5] Herbert Edelsbrunner, David Letscher, and Afra Zomorodian. Topological persistence and simplification. *Discrete & Computational Geometry*, 28(4):511–533, 2002.
- [6] Herbert Edelsbrunner and John Harer. Persistent homology—a survey. In *Surveys on Discrete and Computational Geometry*, volume 453 of *Contemporary Mathematics*, pages 257–282. American Mathematical Society, 2008.
- [7] Herbert Edelsbrunner and John Harer. *Computational Topology: An Introduction*. American Mathematical Society, 2010.
- [8] David Cohen-Steiner, Herbert Edelsbrunner, and John Harer. Stability of persistence diagrams. *Discrete & Computational Geometry*, 37(1):103–120, 2007.
- [9] Ulrich Bauer and Michael Lesnick. Induced matchings and the algebraic stability of persistence barcodes. *Journal of Computational Geometry*, 6(2):162–191, 2015.
- [10] Brittany T. Fasy, Fabrizio Lecci, Alessandro Rinaldo, Larry Wasserman, Sivaraman Balakrishnan, and Aarti Singh. Confidence sets for persistence diagrams. *Annals of Statistics*, 42(6):2301–2339, 2014.
- [11] Frédéric Chazal, Brittany Fasy, Fabrizio Lecci, Bertrand Michel, Alessandro Rinaldo, and Larry Wasserman. Robust topological inference: Distance to a measure and kernel distance. *Journal of Machine Learning Research*, 18(159):1–40, 2018.
- [12] Peter Bubenik. Statistical topological data analysis using persistence landscapes. *Journal of Machine Learning Research*, 16(3):77–102, 2015.
- [13] Henry Adams, Tegan Emerson, Michael Kirby, Rachel Neville, Chris Peterson, Patrick Shipman, Sofya Chepushtanova, Eric Hanson, Francis Motta, and Lori Ziegelmeier. Persistence images: A stable vector representation of persistent homology. *Journal of Machine Learning Research*, 18(8):1–35, 2017.

- [14] Genki Kusano, Kenji Fukumizu, and Yasuaki Hiraoka. Persistence weighted Gaussian kernel for topological data analysis. In *Proceedings of the 33rd International Conference on Machine Learning*, pages 2004–2013, 2016.
- [15] Genki Kusano, Kenji Fukumizu, and Yasuaki Hiraoka. Kernel method for persistence diagrams via kernel embedding and weight factor. *Journal of Machine Learning Research*, 18(189):1–41, 2018.
- [16] Larry Wasserman. Topological data analysis. *Annual Review of Statistics and Its Application*, 5:501–532, 2018.
- [17] Alexander Petersen and Hans-Georg Müller. Fréchet regression for random objects with Euclidean predictors. *Annals of Statistics*, 47(2):691–719, 2019.
- [18] Duligur Ibeling and Thomas Icard. A topological perspective on causal inference. In *Advances in Neural Information Processing Systems 34*, pages 2986–2998, 2021.
- [19] Daisuke Kurisu, Yidong Zhou, Taisuke Otsu, and Hans-Georg Müller. Geodesic causal inference. arXiv:2406.19604, 2024.
- [20] Satarupa Bhattacharjee, Bing Li, Xiao Wu, and Lingzhou Xue. Doubly robust estimation of causal effects for random object outcomes with continuous treatments. arXiv:2506.22754, 2025.
- [21] Kwangho Kim and Hajin Lee. Topological causal effects. arXiv:2603.02289, 2026.
- [22] Amirhossein Farzam, Ahmed Aloui, Vahid Tarokh, and Guillermo Sapiro. Topology-aware robust representation balancing for estimating causal effects. In *ICML 2025 Workshop on High-dimensional Learning Dynamics (HiLD)*, 2025.
- [23] Mouad El Bouchattaoui. Topological residual asymmetry for bivariate causal direction. arXiv:2602.00427, 2026.